GIS-assisted Flood-risk Potential Mapping of Ilorin and its Environs, Kwara State, Nigeria

S. A. Alimi[1,2,3] · E. O. Oriola[4] · S. S. Senbore[5] · V. C. Alepa[2] · F. J. Ologbonyo[2] · F. S. Idris[4] · H. O. Ibrahim[3] · L. O. Olawale[3,6] · O. J. Akinlabi[3,7] · O. Ogungbade[8]

Abstract

The incessant reoccurrence of flooding disasters across Nigeria has mandated an urgent outlook on flood-risk management techniques. Ilorin and its environs have suffered immensely from annual flood reoccurrence. This study aims to assess flood risk within Ilorin and its environs and proffer adequate flood mitigation strategies that governments and policymakers can adopt to placate future flooding events within the state. Satellite imagery data were acquired and analyzed for flood-risk assessment of the area. Ten highly influential flood causative factors were synergized using Multi-Criteria Decision-Making techniques in this research; they are Land Surface Temperature, Elevation, Soil Moisture Index, and Distance to Stream, Drainage Density, Stream Power Index, Normalized Difference Vegetation Index, Land Use Land Cover, Slope, and Topographic Wetness Index. Findings showed that approximately 47.2% of the study area had low flood risk, while moderate and high flood-risk zones occupied 33.5% and 19.29%, respectively. Most parts of Ilorin and its environs are safe from flood disasters; only about one-quarter of the total area under investigation lies in the high flood-risk zones; these areas mostly fall within the shores of major streams, rivers, and dams within the state. A plot of previous flood cases in the state placed the affected areas in the high and moderate zones of flood risk, confirming the efficacy of geospatial techniques in flood-risk assessment. It is hoped that this study's findings and recommendations can be implemented to prevent future devastating flooding occurrences within the state.

✉ S. A. Alimi
alimi.sodiq@gmail.com

1. Faculty of Natural and Agricultural Sciences, Department of Geology, University of The Free State, Bloemfontein, South Africa

2. Faculty of Physical Sciences, Department of Geology and Mineral Science, University of Ilorin, Ilorin, Nigeria

3. College of Science, Engineering and Technology, Department of Geological Sciences, Osun State University, Osogbo, Nigeria

4. Faculty of Social Sciences, Department of Geography and Environmental Sciences, University of Ilorin, Ilorin, Nigeria

5. Faculty of Natural and Agricultural Sciences, Department of Geology, University of Pretoria, Pretoria, South Africa

6. College of Arts and Sciences, Department of Geology, Kansas State University, Manhattan, USA

7. Department of Hydrogeophysics, Nigeria Hydrological Service Agency, Abuja, Nigeria

8. Faculty of Science, Department of Geology, Olabisi Onobanjo University, Ago-Iwoye, Nigeria

1 Introduction

Flooding and flood-related menaces have continuously plagued the global world annually. Of all the natural disasters, flooding has offered the most devastating impact on human existence in recent times [29]. Flooding affects approximately 170 million people annually and has accounted for around 8 million deaths in the past 30 years [2, 55, 57]. Approximately 2.3 billion lives have been swayed by flood impacts, resulting in about USD 386 billion in economic depletion worldwide [23].

Flooding simply means an excessive water flow, which occurs when the water flow velocity is higher than the average volume of a river, usually during episodes of heavy rainfall, dam failures, or melting piles of snow. Flooding is a direct consequence of climate change which affects the entire continent, and this is responsible for the high severity and prevalence of tropical cyclones, typhoons, and hurricanes, as well as various other water-related severe weather spectacles [22, 44]. Extremely high global temperatures facilitate the formation of convection currents, which produce excessive rainfall as its end-product. Global warming is responsible for the continuous melting of ice caps in the polar regions of the world and the consequent global increase in sea levels which contributes to coastal and river flooding [16].

Nigeria is not left out on the list of countries affected by flooding disasters; Nigeria is one of the most affected developing countries in Africa regarding flooding incidences. There is virtually no state in the country that does not experience one or two flooding incidences annually. Over the last ten years, reported flooding cases in Nigeria showed that virtually all the thirty-six states within the country are susceptible to flood disasters [33]. A total of 1550 people died from flooding in 2010, while the disaster displaced approximately 258,000 people [6, 41]. In 2012, 361 lives were lost due to flooding, and 3.8 million people were displaced, costing a total of US$ 6.5 billion in damages [10, 56]. 2015 to 2021 witnessed a far more devastating flooding menace than the previous years, primarily due to the failure of governments and policymakers to learn from past flooding occurrences and the inability to put proper flood forecasting and disaster management systems in place.

The leading mechanisms for flooding in Nigeria include lack of proper drainage systems, inundation of drainage channels because of obstructions, emergency dam releases, and heavy rainfall. Further, rapid population growth, urbanization, and rising sea-levels are the key factors responsible for floods in Nigeria and globally [14, 18].

Ilorin, which is the capital city of Kwara state, north central Nigeria, together with its neighboring towns within the state have continued to witness yearly flooding events. Spontaneous population increase within the state has led to competition for land, increasing waste generation, substandard and limited drainage systems, and poor waste management habits. Flood disasters in the area between the years 1997 and 2021 have mostly occurred within Ilorin, Edu, Patigi, Kpada, Gbogbondogi, Moro, and Lafiaji. Several lives have been lost due to flooding within the state, and multimillion naira worth of properties have been destroyed due to flood disasters [36, 39, 43]. It was reported that flooding in Ilorin city mainly occurs in the rainy season when increased precipitation results in an overflow of water from the Asa River [4, 27] and its tributaries. Effective flood mitigating activities have not been effectively implemented to curb this menace, hence, the yearly reoccurrence of flood disasters within Ilorin.

A major step in mitigating flood occurrences is flood-risk assessment. While several authors have analyzed flooding within the Kwara State [4, 39, 42, 43, 52], there is still inadequacy in the adoption of geospatial (Remote Sensing (RS) and Geographic Information System (GIS)) technology for flood-risk assessment. GIS and RS techniques offer robust flood disaster forecasting and occurrence prediction tools. It has a powerful and reliable tool that provides valuable guidance during discussions aimed at solving flood disasters [12]. Actions geared towards ameliorating flood disasters might only be successful with a proper flood vulnerability map. Several authors have used GIS and RS techniques in flood vulnerability analyses globally [1, 7, 15, 19, 30, 45, 48, 60], and in some parts of the Nigeria [2, 3, 5, 8, 13, 17, 24, 34, 35, 38, 40, 53, 54].

Hence, this present study applied GIS and RS techniques in flood-risk mapping of Ilorin and its environs via Analytical Hierarchy Process (AHP). AHP offers a rapid, cost effective, accurate, and mathematically proven scientific methodologies which are applicable to a wide spectrum of geoscience applications [9]. It is mostly applicable as a first-call tool for a quick delineation and mapping of risk zones in environmental disaster monitoring. For this reason, this method has been adopted in this research and combined with field investigation data for better accuracy. Also, Land Surface Temperature and Soil Moisture Index, which are rarely considered in flood investigations have been applied in this study.

2 Study Area Description

The area of investigation sits within the Nigerian North central geopolitical zone. It covers the City of Ilorin, the capital of Kwara State, and the surrounding major towns that lie within Ilorin South, West and East, Moro, and Asa

Local Government Areas of Kwara State. The study area is sandwiched within latitudes 8°15' and 9°10'North of the Equator and longitudes 4°15' and 4°50′East of the Greenwich Meridian and it has an approximate average altitude value of 300 m (Fig. 1).

Ilorin and environs fall within the transitional zone between savanna and forest regions of Nigeria; it has an annual mean rainfall value of 1200 mm and an average monthly temperature that ranges between 25 °C and 29.5 °C, with March having the highest 30 °C [32]. The study area also forms part of Nigeria's Lower Niger River Basin, covering Kwara state, southern parts of Niger state, and Kogi State. Ilorin area is drained by the tributaries of River Niger in the north and across the western, eastern, and southern margins. Major rivers within the study area include Asa, Agba, Osere, Alalubosa, Okun, and Aluko. Three significant dams exist in the study area: Asa, Agba, and Sobi. According to the National Population Census of 2006 [31], the region's resident population was 1,015,317, and it covered an area of about 3,158.9 km². Oko-Erin, Unity, Bode-Saadu, Ganmo, Fufu, Oke-Oyi, Shao, Idofian, Malete, Alakuko, Oloru, and Onikoko are notable locations within the research area. Geologically, the research area is found in the Southwestern Nigeria's Basement Complex terrain. Igneous and metamorphic rocks such as gneisses, migmatites, granites, quartzites, schists, and amphibolites are the major rock groups in the area.

3 Materials and Method

3.1 Materials

For this investigation, primary and secondary datasets were used. The primary data consists of locations of the places that have flooded within the Ilorin and its environs which was collected using the Global Positioning System (GPS) gadget. The area's Digital Elevation Model (DEM) and LANDSAT 8 Operational Land Imager (OLI) data are the secondary data. Satellite data were acquired from earthexplorer.usgs.gov. Details of the data applied for this research are given in Table 1.

3.2 Method

For a GIS-assisted flood-risk mapping of Ilorin and its environs, ten (10) factors of substantial influence on flooding were considered. The factors are; Land Surface Temperature (LST), Elevation, Soil Moisture Index (SMI), Distance to Stream (DS), Drainage Density (DD), Stream Power Index (SPI), Normalized Difference Vegetation Index (NDVI), Slope, Land Use Land Cover (LULC), and Topographic Wetness Index (TWI). The combined process of flood vulnerability assessment was primarily divided into four
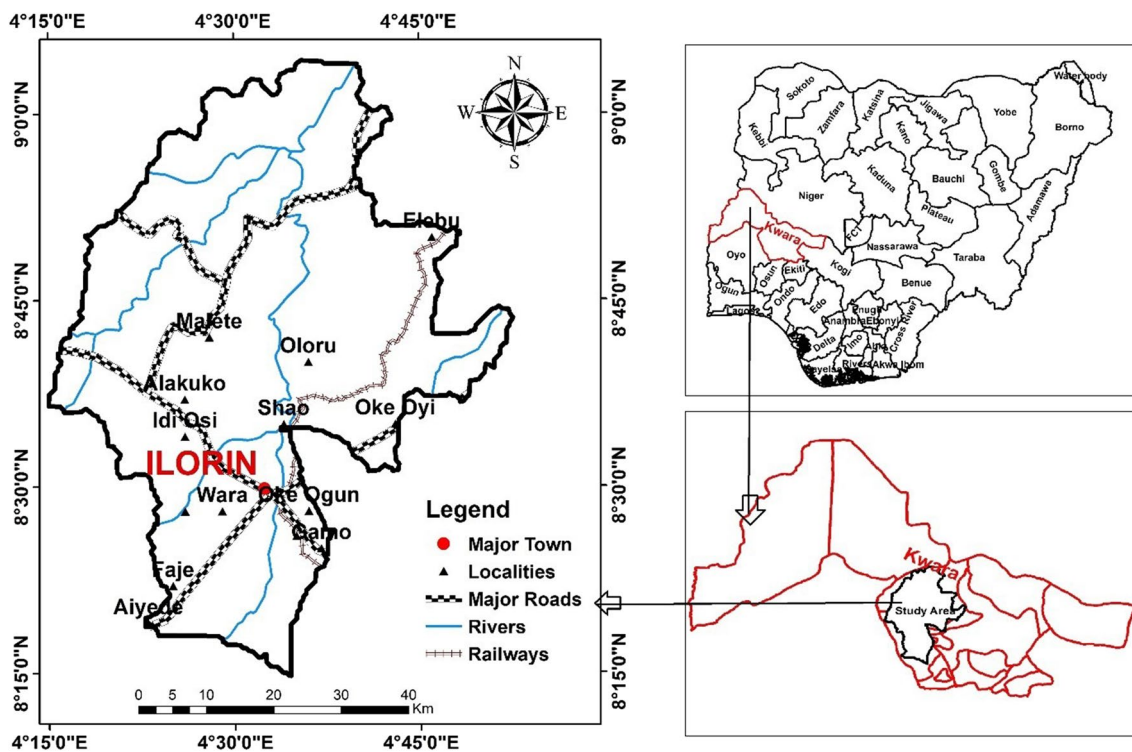

Fig. 1 The study area: Ilorin and its environs

Table 1 Primary and secondary data types and their sources

S/N	Data	Type	Source	Scale
1	Landsat 8 Operational Land Imager (LC08_L1TP_190054_20181225_20190129_01_T1)	Secondary	http://earthexplorer.usgs.gov	30 m
2	SRTM DEM	Secondary	http://earthexplorer.usgs.gov	30 m
3	Coordinates of flood affected areas	Primary	Collected by the Authors with the use of a Global Positioning device	Points

(Fig. 2). Processing and analysis were carried out via the use of GIS and RS software such as ENVI and ArcGIS.

The study area's elevation map was produced via the merged DEM data, elevation map was further used to generate the slope map. Both the elevation and slope maps were further processed to produce SPI and TWI maps. The DD map was computed via streamlines generated from the DEM with the use of ArcHydro tool. DS was also computed using the spatial analyst tool in ArcGIS to buffer areas close to and far away from significant streams. Merged LANDSAT 8 OLI data of the area was processed for basic corrections using ENVI software, and the processed data was used to compute SMI, NDVI, and LST maps. LULC mapping were achieved via a supervised classification technique in GIS.

The classification of the layers and weighting was done using the AHP approach, and the resulting thematic layer maps were created in a pairwise comparison table.

Validation was done by plotting coordinates of affected areas in the state on the output flood-risk map of Ilorin and its environs.

3.3 Mechanisms of Flooding Considered in this Study

3.3.1 Elevation and Slope

The elevation of an area refers to the height to which the area is elevated or rises, usually above sea level. Elevation largely influences the water discharge rate given the fact that water flows downhill from high elevations to low elevations; therefore, areas in low-elevation regions have higher flood risk than high-elevation regions [9, 37]. The slope of an area conveys the landscape steepness in that area. It provides basic information about the
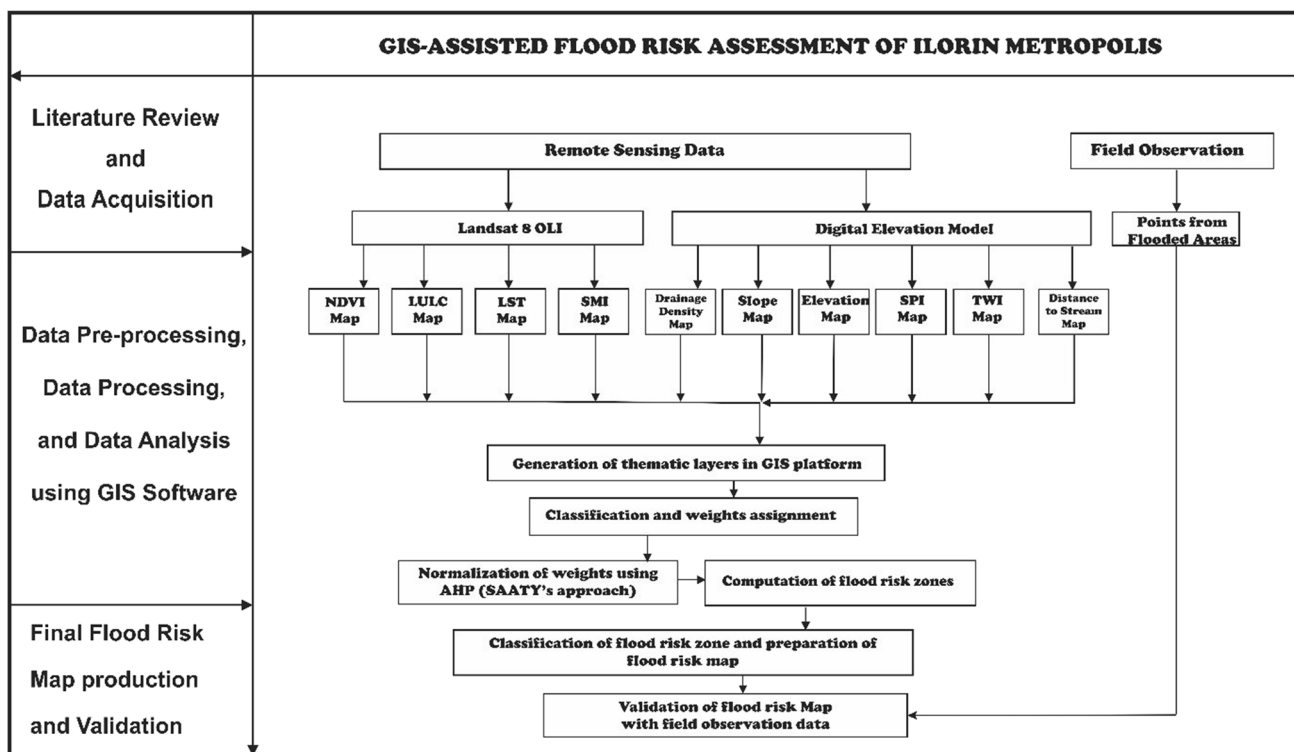
Fig. 2 Stages in flood-risk assessment of Ilorin and its environs

geodynamic processes at work in the area. Slope directly affects water surface discharge and infiltration potency during runoff,therefore, a higher slope leads to rapid runoff and lesser infiltration, while a lower slope contributes to significantly lower runoff and higher infiltration rate during rainfall. Elevation values in the studied part of Ilorin and environs were extracted from the processed SRTM DEM map of the area (Fig. 3a), and ranged from 71 to 566 m. Average elevation value of Osogbo is 320 m [32], therefore, derived elevation values from the DEM map of the study area were divided into five categories: very low elevation (71 m to 203 m), low elevation (203 m to 270 m), moderate elevation (270 m to 321 m), high elevation (321 m to 371 m), and very high elevation (566 m or

above). While 42% of the overall area of focus sits in the high-elevation zones, approximately 58% of it is located in moderate to low-elevation zones. High-elevation places have less of a chance of flooding, while low-elevation areas have a high likelihood of flood threats. Slope angle values were also derived from the SRTM DEM data of the study area using ArcHydro tool in ArcMAP and ranged between 0–36° (Fig. 3b). The slope values were reclassified into five, where 0° to 2° represents a very low slope angle, 2° to 3°, 3° to 6°, 6° to 12°, 12° to 36° signifies low, moderate, high, and very high slope angles, respectively. The moderate and low slope angle zones make up around 85% of the research area, whereas the high slope angle zone makes up 15% (Table 2).
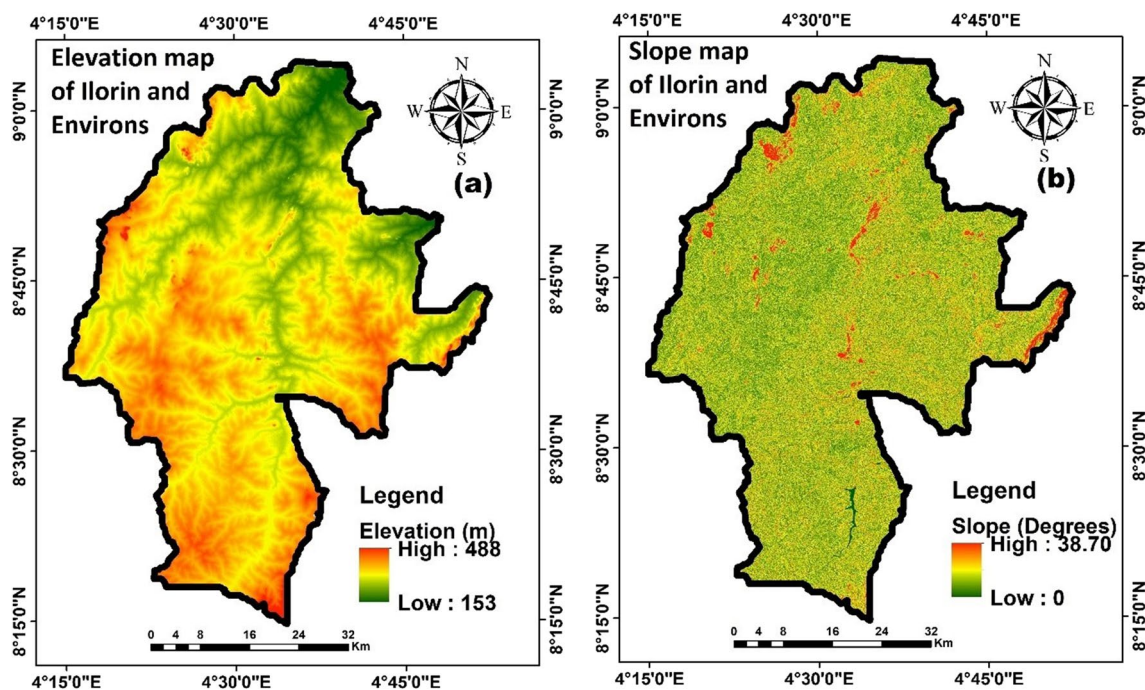

Fig. 3 **a** Map showing elevation variations within Ilorin and its environs, **b** Map showing variation of Slopes angles across the study area

Table 2 Pairwise comparison matrix

Factors	Elevation	Slope	DD	NDVI	LST	SMI	SPI	SD	TWI	LULC	Criteria Weights	Weighted Sums
Elevation	1.00	2.00	2.00	3.00	2.00	2.00	2.00	1.00	3.00	2.00	0.16	1.85
Slope	0.50	1.00	0.50	0.33	0.50	2.00	2.00	0.33	0.50	0.25	0.06	0.65
DD	0.50	2.00	1.00	2.00	0.50	2.00	3.00	2.00	2.00	2.00	0.14	1.49
NDVI	0.33	3.03	0.50	1.00	0.50	1.00	2.00	0.50	3.00	3.00	0.1	1.18
LST	0.50	2.00	2.00	2.00	1.00	2.00	2.00	0.50	2.00	0.33	0.11	1.25
SMI	0.50	0.50	0.50	1.00	0.50	1.00	3.00	0.50	2.00	2.00	0.08	0.94
SPI	0.50	0.50	0.33	0.50	0.50	0.33	1.00	0.50	0.50	0.50	0.05	0.48
DS	1.00	3.03	0.50	2.00	2.00	2.00	2.00	1.00	3.00	2.00	0.14	1.61
TWI	0.33	2.00	0.50	0.33	0.50	0.50	2.00	0.33	1.00	0.50	0.06	0.61
LULC	0.50	4.00	0.50	0.33	3.03	0.50	2.00	0.50	2.00	1.00	0.1	1.18

3.3.2 Drainage Density (DD) and Distance to Stream (DS)

Drainage Density describes the level to which a drainage basin is drained by stream channels and therefore forms a crucial factor in the flood-risk assessment. It is computed by dividing the area of the drainage basin by the total length of all the rivers and streams within the drainage basin. The closer streams are together, the higher the drainage density value; flood danger rises as DD rises and vice versa [20]. The DD map of the focus area (Fig. 4a) was derived from the SRTM DEM data of the area by applying the line density tool on the extracted drainage lines in ArcMAP. Figure 4a shows that DD values ranged from 0 to 0.74 km/km^2. While only 26% of the area under investigation has high to very high DD, the remaining 74% has moderate to low DD values (Table 2), which is anticipated to increase floods during periods of severe rainfall. The chance of flooding in a location after a heavy downpour is also influenced by how far away it is from a big stream [50]. Because river-induced floods occur more frequently and with greater intensity closer to the drainage line, considering the closeness of streams is essential when determining flood risk. DS was computed using Euclidean distance tool in ArcMAP with a maximum allowed distance of 2 km. Areas between 0 to 0.2 km of major streams are considered close to a major stream, while areas between According to the study area's DS map (Fig. 4b), 46% of the area is close to a major stream and has a high risk of flooding, while the remaining 54% is far away and has a reduced risk of flooding.

3.3.3 TWI (Topographic Wetness Index) and SPI (Stream Power Index)

TWI demonstrates the regional distribution of wetness, soil moisture, saturation zone, groundwater level, and flow aggregation. A high TWI rating implies wet, extremely susceptible to flooding land. Equation 1 below was used to compute the TWI (after [11]:

$$TWI = \ln(\frac{\alpha}{tan\beta}) \tag{1}$$

where $tan\,\beta$ is the slope angle at the location and α represents the total upslope area draining via a single spot (per unit contour length). Compared to 19% of the area, which has high TWI values and is likely prone to flooding, 81% of the Ilorin and its environs have low TWI values and less likely to flood during periods of severe rainfall (Fig. 5a). SPI describes the volume of water flowing over a watershed as contrasted to TWI [47]. It illustrates how frequently flooding occurs. Low SPI levels indicate minimal to no downstream water movement, which is more likely to cause floods, while high SPI values suggest swift downstream water flow which implies low flood danger.

$$SPI = As tan\beta \tag{2}$$

where β is the slope radiant (in °), and As depicts the catchment area (in m^2 m^{-1}). The SPI map (Fig. 5b) for the study area was segmented into five (5) groups, with low SPI accounting for 98% of the region. As a result of the
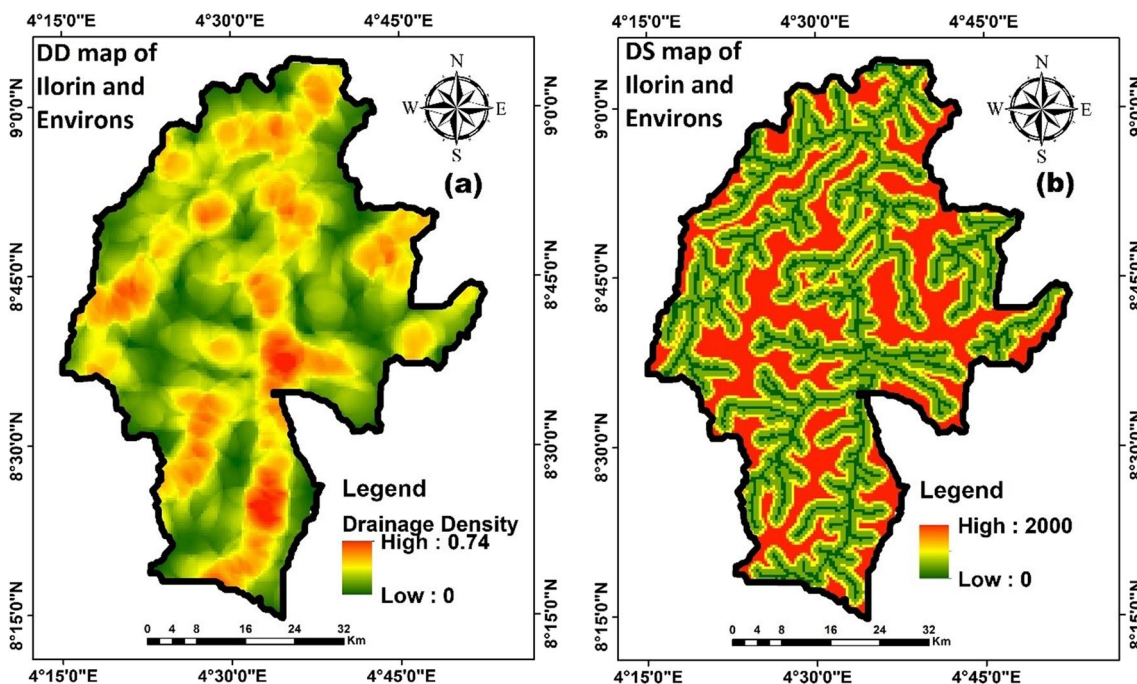

Fig. 4 **a** Drainage Density distribution within the study area, **b** Distance to Streams (m) variation in the study area
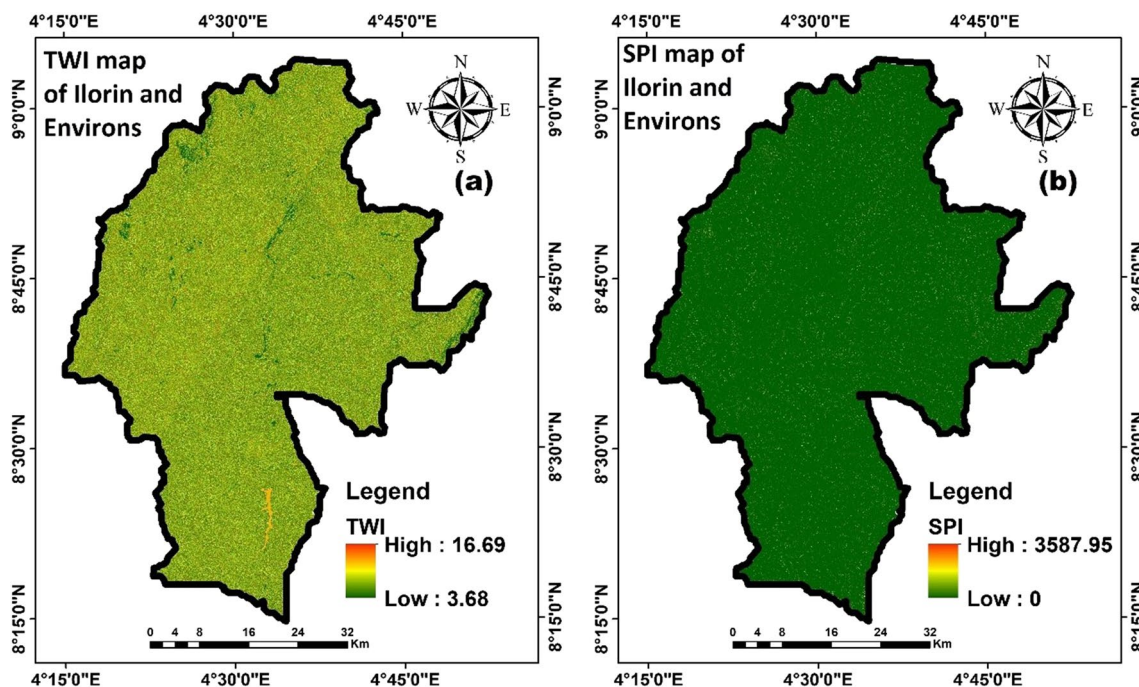
Fig. 5 **a** Topographic Wetness Index variation in the study area, **b** Power Index of streams within Ilorin and its environs

remaining 2%'s high SPI, the majority of the locations have low SPI values and are vulnerable to flooding.

3.3.4 Normalized Difference Vegetation Index (NDVI) and Land Use Land Cover (LULC)

NDVI map displays precise locations of areas with thriving vegetation and areas with little or no vegetation; this is important in flood-risk assessment because vegetation influences water movements, making it a conservational property of flooding, which is useful when assessing plant communities' growth and development [9, 46]. NDVI values generally vary between -1 and +1. NDVI was computed using Eq. 3:

$$NDVI = \frac{(NIR - R)}{(NIR + R)} \tag{3}$$

where R represents Red bands (Band 4 in Landsat 8), and NIR indicates Near Infrared Red bands (band 5 in Landsat 8).

Zero and negative NDVI values show water and barren land, NDVI values between 0.2 to 0.4 show grassland, while > 0.5 represent forest land [26]. NDVI map of Ilorin and its environs (Fig. 6a) showed that the Vegetation index is high in most of the remote parts of the studied area, hence a low likelihood of flooding. Low indices are seen in the built-up parts of Ilorin, where industrializations are taking place, these areas have little to no vegetation within them that can slow down water movement during excess rainfall and hence, have a high flood risk.

Another critical factor for consideration in flood-risk assessment is LULC; it controls the rate of infiltration of surface and groundwater on land. Vegetated and open land permit easy flow and infiltration of water, thereby reducing flood risk, while built-up areas do not, increasing flood risk. LULC map of Ilorin and its environs was derived from the area's Landsat 8 data using the Maximum Likelihood technique in GIS. Equation 4 [25] was used to calculate the output accuracy as follows:

$$\text{Overall accuracy (OA)} = \frac{\text{No. of correct observations}}{\text{Total no. of observations}} \tag{4}$$

$$\text{OA} = \frac{71}{80} = 88.7\%$$

Observation data were derived from field investigation across the study area. This was done to ascertain the LULC pattern on ground in the study area.

A multivariate technique called kappa (k) analysis uses Khat statistics, which indicate the degree of accuracy, to assess output map accuracy levels. The Kappa coefficient was compiled using Eq. 5 [37, 58].

$$K = \frac{\% \text{ overall correct value } - \% \text{ correct agreement to observed values}}{\text{Total no. of class } - \% \text{ correct agreement to observed values}} \tag{5}$$

An overall accuracy (OA) value of 88.7% suggests a strong association. The calculated Kappa coefficient (K) value was 0.82, which further demonstrates the overall precision of the observed LULC in the research area. Five
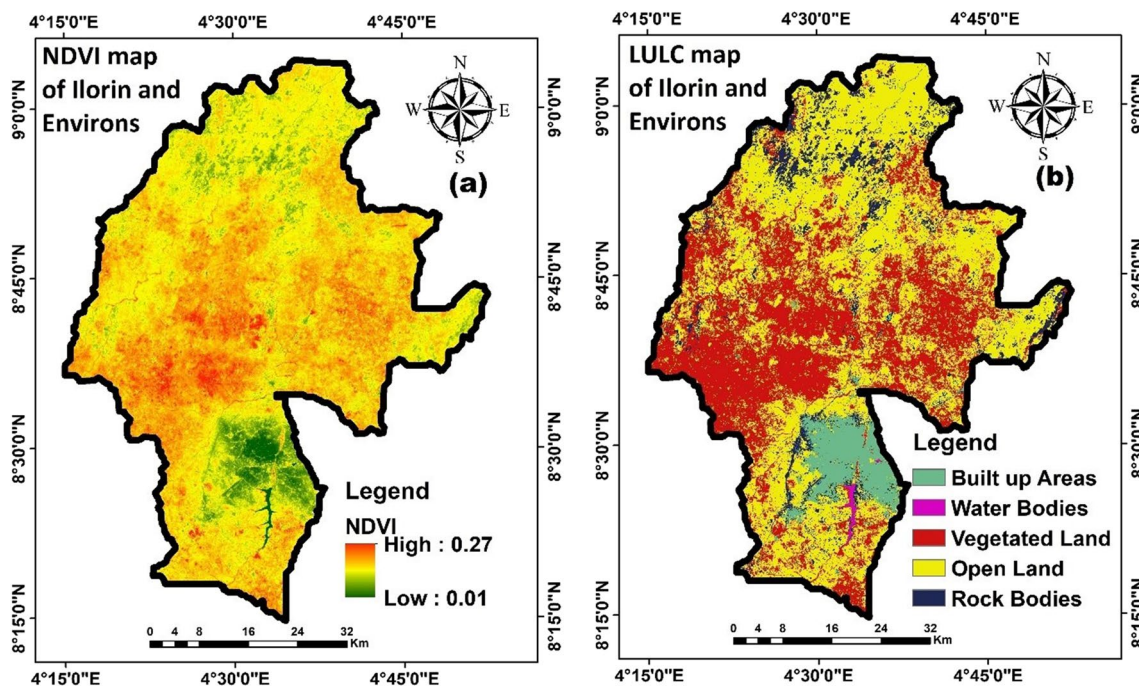
Fig. 6 **a** Normalized Difference Vegetation Index variation across Ilorin and its environs, **b** Land Use and Land Cover types in the study area

categories were identified from the LULC map of Ilorin and its environs (Fig. 6a): open/barren land, built-up regions, vegetated land, water bodies, and rocky areas. Open/bare land makes up 52.5% overall, followed by vegetated land (34.4%), rocky terrain (9.8%), built-up regions (3.8%), and water bodies (0.25%). While vegetation-covered and rocky locations are least harmed by floods, they mostly affect built-up regions and bodies of water.

3.3.5 LST (Land Surface Temperature) and SMI (Soil Moisture Index)

LST is one factor rarely used in flood-risk assessment. It gauges the amount of thermal radiation that is emitted from the ground when sun energy interacts with and warms the bare earth or vegetation [21]. LST is a crucial tool in studying the physical processes of the land surface,it provides insight into how LST variation influences hydrological and meteorological systems in an area, hence its application in flood-risk potential assessment. As the average temperature of land increases, more evaporation occurs, leading to an increase in overall precipitation. Urban areas are characterized by high surface temperatures, while water bodies and vegetated lands have low LST. Thermal Infrared Sensor (TIR) band of Landsat 8 was used as an input band together with K_1 and K_2 values provided in the Landsat 8 metadata. LST was computed in ArcMap using Eq. 6. The Landsat 8 data was acquired in the month of December 2018 when vegetation is less abundant.

$$LST = \frac{BT}{1 + w} \times \frac{BT}{p} \times In(e) \qquad (6)$$

BT represents At-Sensor brightness temperature, w represents λ of emitted radiance,

p is calculated as $h \times \frac{c}{s}(1.438 \times 10^{-2} mK)$

H   is the Plank's constant which is $6.626 \times 10^{-34} Js$
S   represents Boltzmann constant which is $1.38 \times 10^{-23} J/K$
C   represents speed of Light which is $2.998 \times 10^8 m/s$
e   Land Surface Emissivity

The LST values in the area (Fig. 7a) ranged from 60 °C to 73 °C. While 47% of the whole research area has an LST value between low and very low, approximately 53% of it falls between moderate and very high.

SMI is another factor rarely used in the flood-risk potential assessment. The ratio of the difference between the current soil moisture and the permanent wilting point to the field capacity and the remaining soil moisture is known as the SMI. This index varies from 0 to 1, where 0 signifies exceptionally dry soil and 1 denotes exceptionally wet soil conditions [49]. The soil's wet condition indicates the soil's ability to hold water during runoff, which helps reduce flooding. In contrast, dry soil conditions show the soil's inability to retain water, thereby contributing to flooding. Figure 7b shows the SMI map of Ilorin and its environs,
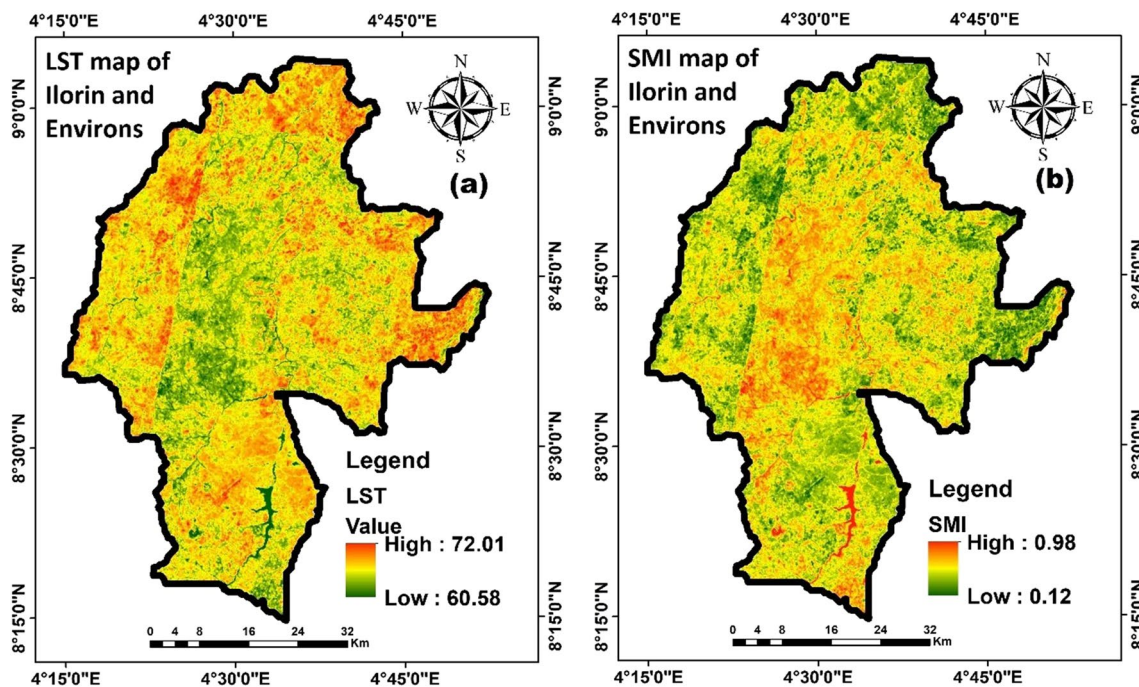
Fig. 7 **a** Land Surface Temperature pattern within Ilorin and its environs, **b** Soil Moistures Index variations in the study area

74% overall falls in the moderate and low SMI, and 26% falls in the high soil moisture index. SMI was computed using Eq. 7 (after [59]).

$$SMI = \frac{(LSTmax - LST)}{(LSTmax - LSTmin)} \tag{7}$$

where LSTmin is the minimum LST of a given NDVI, and LSTmax is the maximum LST of a given NDVI.

A comparison between SMI and LST shows that areas with high LST have low SMI, while areas with low LST have high SMI; this implies that as surface temperature increases in soils, moisture level reduces because water is lost to the atmosphere during evaporation. Soils with good water retention capacity will retain some excess water during heavy rainfall, thereby limiting the effect of flooding. In contrast, dry soils tend to be soggy and flooded during excess rainfall.

3.4 Determining Criteria Weight

One of the key methods for Multi-Criteria Decision Making's (MCDM) balancing is AHP, which was developed by Saaty [51]. The MCDM technique helps compare various factors simultaneously via a matrix of pairwise comparison that orders the proportionate influence of one criterion over another. The importance ranking runs from 1 to 9, where 9 denotes the greatest significance and 1 denotes the equal significance. Due to the AHP method's effectiveness in this aspect, it is applicable in various industries globally, including transportation, education, and healthcare [28].

The Analytical Hierarchy Process (AHP) makes it possible to arrange criteria hierarchically and contributes to the extent of logical reasoning supported by a conceptual model [50]. The pairwise comparison matrix (Table 2) was computed based on relative scale of importance. It was further normalized to derive the Criteria Weights (CW) and Weighted Sums (WS). Equation 8 was used to determine the Consistency Index (CI), while Eq. 9 was used to derive the Consistency Ratio (CR).

$$CI = \frac{\lambda_{max} - k}{k - 1} \tag{8}$$

$$CR = \frac{CI}{RI} \tag{9}$$

The calculated CR for the study area was 0.09, while the CI was 0.12. A consistency ratio value < 1 implies a logical perception, but when it is > 0.1, the assessment needs to be amended. The AHP readings are consistent because the CR value is within the permitted range.

By using a weighted index overlay to combine all the thematic layers, a flood-risk map was produced (Eq. 10).

$$Flood - risk\ map\ (FR) = \sum_{i,j=1}^{8} WiXj \tag{10}$$

where; Wi = % weight thematic map

Table 3 Weight assessment and arrangement for flood-risk mapping

| Factor	Categories	Influence	Rankings	Area covered in Km^2	% Area covered	Criteria Weights
Altitude	71–203	Very High	9	296.89	9.40	16
	203–270	High	7	685.04	21.69	
	270–321	Moderate	5	899.83	28.49	
	321–371	Low	3	843.78	26.71	
	371–566	Very Low	1	433.35	13.72	
Slope	0–2	Very High	9	953.33	30.18	6
	2–3	High	7	1294.79	40.99	
	3–6	Moderate	5	752.03	23.81	
	6–12	Low	3	139.49	4.42	
	12–36	Very Low	1	19.28	0.61	
LULC	Water Body	Very High	9	6.75	0.21	10
	Built-up Lands	High	7	166.20	5.26	
	Open/Barren Land	Moderate	5	1605.96	50.84	
	Vegetated Land	Low	3	1133.99	35.90	
	Rocky Areas	Very Low	1	246.04	7.79	
DD	0.46–0.74	Very High	9	319.42	10.11	14
	0.35–0.46	High	7	655.06	20.74	
	0.23–0.35	Moderate	5	706.44	22.36	
	0.12–0.23	Low	3	776.77	24.59	
	0–0.12	Very Low	1	701.16	22.20	
SPI	6478–27082	Very High	9	1.64	0.05	5
	849–6478	High	7	11.12	0.35	
	212–849	Moderate	5	49.26	1.56	
	0–212	Low	3	223.16	7.06	
	0	Very Low	1	2873.74	90.97	
TWI	10.80–19.05	Very High	9	162.13	5.13	6
	9.11–10.80	High	7	315.33	9.98	
	7.72–9.11	Moderate	5	513.87	16.27	
	6.70–7.72	Low	3	1148.91	36.37	
	3.68–6.70	Very Low	1	1018.67	32.25	
DS	0–396	Very High	9	425.89	13.48	14
	396–793	High	7	1113.77	35.26	
	793–1189	Moderate	5	537.06	17.00	
	793–1586	Low	3	137.15	4.34	
	1586–1982	Very Low	1	944.98	29.92	
NDVI	-0.08—0.02	Very High	9	377.5	11.95	10
	0.02—0.1	High	7	993.44	31.45	
	0.1–0.12	Moderate	5	1117.55	35.38	
	0.12–0.15	Low	3	515.32	16.31	
	0.15–0.27	Very Low	1	155.12	4.91	
LST	68.48–73.66	Very High	9	9.59	0.30	11
	67.54–68.48	High	7	492.01	15.58	
	66.60–67.54	Moderate	5	981.93	31.08	
	64.98–66.60	Low	3	1099.96	34.82	
	60.33–64.98	Very Low	1	575.44	18.22	
SMI	0–0.38	Very High	9	10.14	0.32	9
	0.38–0.45	High	7	612.45	19.39	
	0.45–0.52	Moderate	5	1049.03	33.21	
	0.52–0.64	Low	3	1036.78	32.82	
	0.64–1.0	Very Low	1	450.53	14.26	
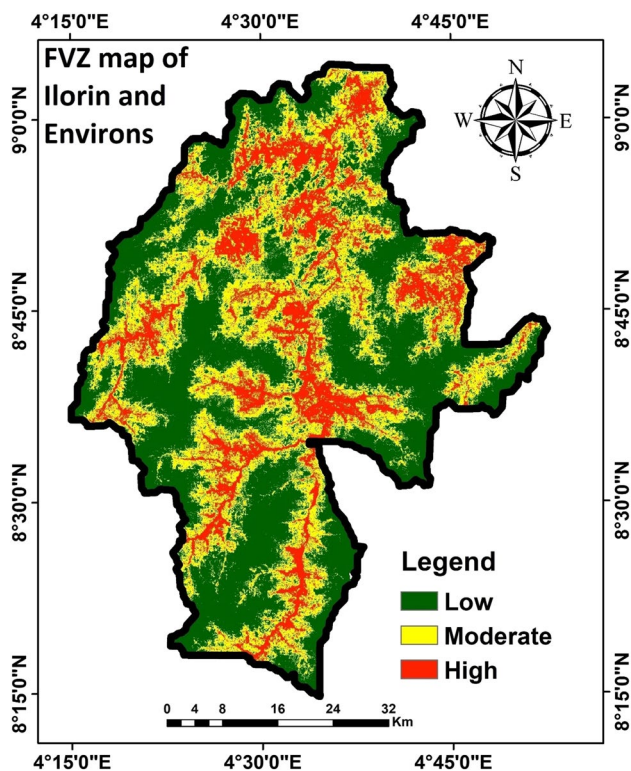
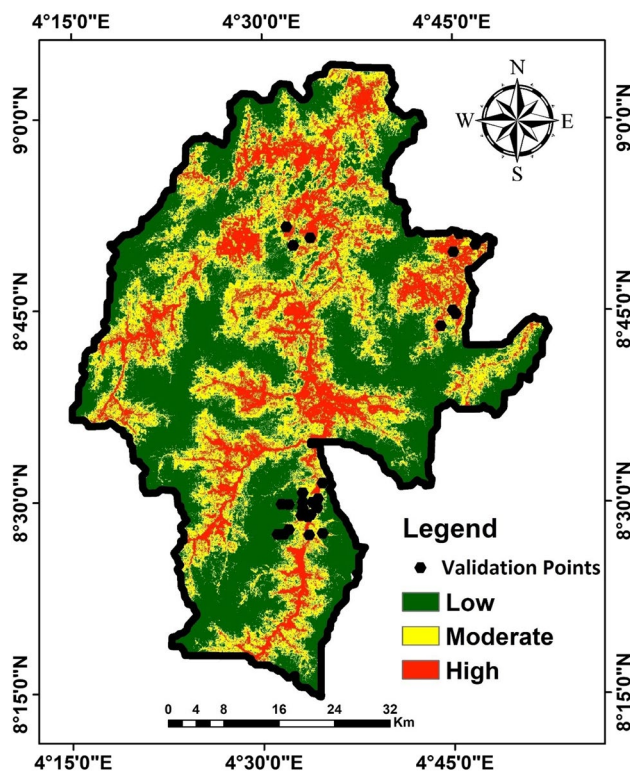**Fig. 8** Flood-risk map of Ilorin and its environs

Fig. 9 Validation points on Flood-Risk map of Ilorin and its environs

Table 4 Flood-risk level with areal extent

Flood-risk level	Flood-risk index	Area (Km²)	% Coverage
Low	1–2	1491.07	47.2
Moderate	3	1058.25	33.5
High	4–5	609.59	19.29

Xj = reclassified map

Weight assignment and arrangement for the prepared thematic layers for flood-risk assessment are given in Table 3. The ten (10) flood causative factors considered in the study were reclassified into 5 groups, where 1 represents low flood-risk and 9 represents high flood-risk. The thematic maps were rescaled and reclassified into equal spatial resolution for better accuracy. Weight assignment and classifications were based on expert opinions, literature study, and previous works on similar methodology. Processing was done in a GIS environment. The layer values were classified into five categories based on influence on flood-risk which varies from very low to very high. The area covered by each category is also given in percent and kilometers.

4 Results and Discussion

4.1 Flood-Risk Zones Mapping

The primary motive for flood-risk assessment is to produce a map showing the various areas with high and low flood risks within an area. The ten flood factors were merged via Weighted Overlay Index in ArcMAP to produce the flood-risk map of Ilorin and its environs. The output flood-risk map (Fig. 8) showed the flood-risk zonation pattern in Ilorin area. The flood-risk map was categorized into three viz-a-viz low, moderate, and high flood-risk zones. Areas with flood-risk index of 1 to 2 are classified as low, while 3 and 4 to 5 are classified as moderate and high, respectively. Table 4 shows the areal coverage of each zone. It can be observed that 12.49% of the total landmass under investigation lies in the high flood-risk zone, while 54.69% and 32.82% sit in the low and moderate flood-risk zones, respectively. The majority of the area of study is located within the moderate and low flood-risks zones. The regions with a high danger of flooding are those that are near large streams, waterways, and dams.

During times of heavy rainfall or flooding, communities located in high flood-risk zones are expected to suffer significantly. Additionally, places with low and extremely low

Table 5 Error matrix of flood-risk map in Ilorin and environs

S/n	Flood-risk levels	Low	Moderate	High	Total	Correct points
1	Low	6	0	0	6	6
2	Moderate	0	15	4	19	15
3	High	0	4	31	35	31
	Total	6	19	35	60	52

flood risks have a lower likelihood of experiencing flooding. When determining flood risk, elevation and distance from streams are important considerations. High flood-risk zones as indicated on the flood-risk map are areas with low elevation and closer to major streams. Further, drainage density values are also high in high flood-risk areas. High LST and SMI values also contributed to the increased flooding in these areas. Low flood-risk areas are mainly within the high-elevation regions and farther away from major streams; drainage density values are also low in such areas.

4.2 Validation of Flood Vulnerable Zones Map

Sixty (60) points were collected from areas of reported flood and no flood occurrences within the studied part of the Ilorin and environs to validate the flood-risk map produced. To determine the level of accuracy of the findings, these sites were overlaid on the flood-risk map generated. Figure 9 shows the plots of the reported flood cases across Ilorin on the flood-risk map of Ilorin and its environs. It can be observed that the majority of the reported incidences, which span the years 2011 to 2021, mainly fell within moderate and high flood-risk zones on the map; this confirms the validity of the findings of this research. Further, points collected from flood affected areas and areas of little or no flooding events were computed to access the overall accuracy of the output Flood-Risk map. The error matrix details are given in Table 5; the Overall Accuracy (OA) and Kappa coefficient (K) value were derived as 86.7% and 81%, respectively.

5 Discussion

Identification of flood-vulnerable zones using GIS and RS techniques has significantly contributed to flooding mitigation strategies in recent years. From the results of this research, the ten flood causative factors all played different roles in the intensity and frequency of flooding that has continued to ravage Ilorin and its environs. Table 3 revealed that 33.5% and 19.29% of the study area are in moderate and high flood-risk zones, respectively, while 47.2% of the region is in a low flood-risk zone. The studied part of Ilorin lies on a relatively high-elevation terrain, which is why most places away from the major streams have a low flood risk. Most areas affected across the states are areas close to major streams; a heavy downpour of rainfall brings about overflow of these streams flowing through culverts and drainage channels. This overflow makes its way into nearby residents, especially houses within a 500 m radius of the major streams. Elevation and slope angles affect the rate of movement of excess water from the stream channels. The low elevation along the river channels and low slope angles makes it easy for water to find their ways to residential areas as water moves from high heights too low land areas. Vegetation indices, soil moisture index, and land surface temperatures are factors that have moderate effects on the control of flooding. In contrast, topographic wetness and stream power indices have minimal control over flooding in the area. Several dams within the study area have been reported to be a major contributing factor to flooding within Ilorin and its environs [42]. Asa dam is located within Ilorin and overflows from the dam during excess water control floods nearby residents. Alimi et al. [9] have previously recommended GIS as a practical tool for flood-risk mapping, their study also showed that distance to streams and elevation are highly influential flood causative factors, this is similar to the results derived in this present study. Oriola and Chibuike [43] also reported in part of Kwara state, that distance to major drainage channels affect flooding within the state. Other factors such as precipitation and socioeconomic status were also recommended by Hussain et al. [23]. In the present study, elevation, distance to stream, and drainage density, as seen in Table 3, are the most influential flood-risk factors in the study area.

The ability to visualize flood-risk zones makes mitigation strategies and planning an easy task. The importance of a flood-risk map in conversations geared towards ameliorating flooding incidences cannot be overemphasized. In the present study area, there is a pressing call for genuine land use control strategies. Land acquisition in high flood-risk zones needs to be controlled; this will cushion the yearly loss of life and properties that arise during flooding events. Further, the construction of river embarkments along stream channels can prevent water overflow to residential areas during periods of excessive rainfall. The embarkments will control the movement of water and slow the rate of excessive spreads into the residential areas. Also, there is an urgent need for flood warning systems that alert people to the likelihood of a flood in the future; this will enable proper preparations and prevents sudden loss of life and properties.

6 Conclusions and Recommendation

The seasonal reoccurrence of flooding within Ilorin, the Kwara state capital, mandated the urgent need for flood-risk assessments in some parts of the state. Flood-risk potential assessment is a useful pre-disaster management technique, especially when assessing the risk of flooding in an area against all flooding mechanisms, such as groundwater, pluvial, fluvial, and tidal. It also involves flood mitigation measures. Most parts of Ilorin and its environs are within the low flood-risk zones, and areas of high flood occurrence are extremely close to major river channels that tend to overflow during periods of heavy downpours. This could have been averted by preventing land acquisition near the rivers. GIS and remote sensing techniques offer cheap and user-friendly practical flood-risk mapping tools, which can be used to map flood-risk zones quickly. This is effective in this study. The MCDA technique might go a long way in providing valuable information for effective flood mitigation controls. To avoid occupying high flood-risk lands, It is strongly advised that locals be actively discouraged from erecting homes close to important waterways. Additionally, the government needs to install proper flood warning systems and flood-resistant buildings throughout flood-prone locations.

Declarations

Competing Interests The authors have no competing interest to declare.

References

1. Abdalla R, Li J (2010) Towards effective application of geospatial technologies for disaster management. Int J Appl Earth Obs Geoinformation 12:405–407
2. Adebayo HO (2016) GIS analysis of flood vulnerable area in Benin-Owena River Basin Nigeria. Indones J Geogr 49(1):27–33
3. Adefisan EA, Bayo AS, Ropo OI (2015) Application of Geo-Spatial technology in identifying areas vulnerable to flooding in Ibadan Metropolis. J Environ Earth Sci 5:156–165
4. Adeniran KA, Ottawale YA, Ogunshina MS (2018) Mapping and evaluation of flood risk areas along Asa River using remote sensing and GIS techniques. FUOYE J Eng Technol 3(2):12–16
5. Adetoro OO, Akanni O (2018) Flood vulnerability assessment in Ilaje, Ondo State, Nigeria. J Geogr, Environ Earth Sci Int 16(1):1–11
6. Agboola BS, Ajayi O, Taiwo OJ, Wahab BW (2012) The August 2011 flood in Ibadan, Nigeria: Anthropogenic causes and consequences. Int J Disaster Risk Sci 3:207–217
7. Albano R, Sole A, Adamowski JF, Perrone A, Inam A (2018) Using FloodRisk GIS freeware for uncertainty analysis of direct economic flood damages in Italy. Int J Appl Earth Obs Geoinformation 73:220–229
8. Alimi SA, Ige OO, Okeke JC (2022) Assessing groundwater potentials of Kaduna State, Northwestern Nigeria, using geographic information system (GIS) and remote sensing (RS) techniques. Arab J Geosci 15:1741
9. Alimi SA, Andongma TW, Ogungbade O, Senbore SS, Alepa VC, Akinlabi OJ, Olawale LO, Muhammed QO (2022) Flood vulnerable zones mapping using geospatial techniques: Case study of Osogbo Metropolis Nigeria. Egypt J Remote Sens Space Sci 25:841–850
10. Amangabra G, Obenade M (2015) Flood vulnerability assessment of Niger Delta states relative to 2012 flood disaster in Nigeria. Am J Environ Protection 3(3):76–83
11. Chapi K, Singh VP, Shirzadi A, Shahabi H, Bui DT, Pham BT, Khosravi K (2017) A novel hybrid artificial intelligence approach for flood susceptibility assessment environ. Model Softw 95:229–245
12. Chohan K, Ahmad SR, Ashraf A, Kamran M, Rasheed R (2022) Remote sensing based innovative solution of river morphology for better flood management. Int J Appl Earth Obs Geoinformation 111:102845
13. Chukwuma EC, Okonkwo CC, Ojediran JO, Anizoba DC, Ubah JI, Nwachukwu CP (2021) A GIS based flood vulnerability modelling of Anambra State using an integrated IVFRN-DEMATEL-ANP model. Heliyon 7(9):e08048
14. Cirella GT, Iyalomhe FO (2018) Flooding conceptual review: sustainability-focalized best practices in Nigeria. Appl Sci 8(9):1558
15. Danumah JH, Odai SN, Saley B, Szarzynski J, Thiel M, Kwaku A, Kouame F, Akpa LY (2016) Flood risk assessment and mapping in Abidjan district using multi-criteria analysis (AHP) model and geo-information techniques, (cote d'ivoire). Geoenviron Disasters 3:1–13
16. Deepak S, Rajan G, Jairaj PG (2020) Geospatial approach for assessment of vulnerability to flood in local self-governments. Geoenviron Disasters 7:1–19
17. Dutal H (2023) Determining the effect of urbanization on flood hazard zones in Kahramanmaras, Turkey, using flood hazard index and multi-criteria decision analysis. Environ Monit Assess 195:92
18. Echendu AJ (2020) The impact of flooding on Nigeria's sustainable development goals (SDGs). Ecosyst Health Sustain, Taylor and Francis 6(1):1791735
19. Gan TY, Zunic F, Kuo CC, Strobl T (2012) Flood mapping of Danube River at Romania using single and multi-date ERS2-SAR images. Int J Appl Earth Obs Geoinformation 18:69–81

20. Ghodratabadi S, Feizi F (2015) Identification of groundwater potential zones in Moalleman, Iran by remote sensing and index overlay technique in GIS. Iran J Earth Sci 7:142–152

21. Glynn CH, Darren G (2019) Taking the temperatures of the earth. Elsevier, pp 57–127

22. Hall J, Arheimer B, Borga M, Brázdil R, Claps P, Kiss A, Llasat MC (2014) Understanding flood regime changes in Europe: A state of the art assessment. Hydrol Earth Syst Sci 18(7):2735–2772

23. Hussain M, Tayyab M, Zhang J, Shah AA, Ullah K, Mehmood U, Al-Shaibah B (2021) GIS-based multi-criteria approach for flood vulnerability assessment and mapping in district Shangla: Khyber Pakhtunkhwa. Pak Sustain 13:3126

24. Isma'il M, Saanyol IO (2013) Application of remote sensing (RS) and geographic information systems (GIS) in flood vulnerability mapping: Case study of River Kaduna. Int J Geomatics Geosci 3:618–627

25. Jensen JR (1996) Introductory Digital Image Processing: A Remote Sensing Perspective, 2nd edn. Prentice Hall Inc, Upper Saddle River NJ

26. Khosravi K, Shahabi H, Pham BT, Adamowski JF, Shirzadi A, Pradhan B, Dou J, Ly H, Gróf G, Ho HL, Hong H, Chapi K, Prakash I (2019) A comparative assessment of flood susceptibility modeling using multi-criteria decision-making analysis and machine learning methods. J Hydrol 573:311–323

27. Kolawole OM, Olayemi AB, Ajayi KT (2011) Managing flood in Nigerian cities: Risk analysis and adaptation options – Ilorin city as a case study. Arch Appl Sci Res 3(1):17–24

28. Majumder M (2015) Impact of urbanization on water shortage in face of climatic aberrations. Springer, pp 35–47

29. Matgen P, Schumann GJ, Henry J, Hoffmann L, Pfister L (2007) Integration of SAR-derived river inundation areas, high-precision topographic data and a river flow model toward near real-time flood management. Int J Appl Earth Obs Geoinformation 9:247–263

30. Mujib M, Apriyanto B, Kurnianto F, Ikhsan F, Nurdin E, Pangastuti E, Astutik S (2021) Assessment of flood hazard mapping based on Analytical Hierarchy Process (AHP) and GIS: Application in Kencong District, Jember Regency, Indonesia. Geosfera Indones 6:353–376

31. National Population Commission (NPC) (2006) Nigeria National Census: population distribution by sex, State, LGAs and Senatorial District: 2006 census priority tables (vol 3)

32. Nigerian Meteorological Agency (NiMET) (2021) Seasonal rainfall prediction. Available at https://nimet.gov.ng/publication/2021-seasonal-rainfall-prediction Accessed 10 Jun 2021

33. Nigerian Meteorological Agency (NiMET) (2022) Seasonal rainfall prediction. Available at https://nimet.gov.ng/publication/2022-seasonal-rainfall-prediction Accessed 19 Jul 2022

34. Ndidi NF, Innocent BE, Ganiy AI (2022) Flood risk mapping and urban infrastructural susceptibility assessment using a GIS and analytic hierarchical raster fusion approach in the Ona River Basin, Nigeria. Int J Disaster Risk Reduction 77:103097

35. Nkeki FN, Henah PJ, Ojeh VN (2013) Geospatial techniques for the assessment and analysis of flood risk along the Niger-Benue Basin in Nigeria. J Geogr Inf Syst 5:123–135

36. Ogunbodede EF, Sunmola RA (2014) Flooding and traffic management in Akure (Nigeria) metropolitan environment. Eur Environ Sci Ecol J 1(2):24–38

37. Ogungbade O, Ariyo SO, Alimi SA, Alepa VC, Aromoye SA, Akinlabi OJ (2022) A combined GIS, remote sensing and geophysical methods for groundwater potential assessment of Ilora, Oyo Central, Nigeria. Environ Earth Sci Springer 81:74

38. Okonufua E, Olajire OO, Ojeh VN (2019) Flood vulnerability assessment of Afikpo South Local Government Area, Ebonyi State, Nigeria. Int J Environ Clim Change 9(6):331–342

39. Olabode AD, Ajibade LT, Yinusa O (2014) Analysis of flood risk zones (Frzs) around Asa River in Ilorin using geographic information system (GIS). Int J Innov Sci, Eng Technol 1(9):1–8

40. Olii MR, Olii A, Pakaya R (2021) The integrated spatial assessment of the flood hazard using AHP-GIS: The case study of Gorontalo regency. Indones J Geogr 53(1):126–35

41. Oluwaseyi AB (2017) Plant genetic resources (PGR) in Nigeria and the reality of climate change: A review. Asian J Environ Ecol 2:1–24

42. Oriola E, Bolaji S (2012) Urban flood risk information on a River Catchment in a Part of Ilorin Metropolis, Kwara State, Nigeria. IISTE J 2(8):70–83

43. Oriola EO, Chibuike CC (2016) Flood risk analysis of edu local government area (Kwara State Nigeria). Geogr, Environ, Sustain 9:106–116

44. Ouma YO, Tateishi R (2014) Urban flood vulnerability and risk mapping using integrated multi parametric AHP and GIS: methodological overview and case study assessment. Water 6(6):1515–1545

45. Ozkan SP, Tarhan C (2016) Detection of flood hazard in urban areas using GIS: Izmir case. Procedia Technol 22:373–381

46. Pal SC, Chakrabortty R, Malik S, Das B (2018) Application of forest canopy density model for forest cover mapping using LISS-IV satellite data: a case study of Sali watershed, West Bengal. Model Earth Syst Environ 4:853–865

47. Poudyal CP, Chang C, Oh HJ, Lee S (2010) Landslide susceptibility maps comparing frequency ratio and artificial neural networks: a case study from the Nepal Himalaya. Environ Earth Sci 61:1049–1064

48. Rincón D, Khan UT, Armenakis C (2018) Flood risk mapping using GIS and multi-criteria analysis: A greater Toronto area case study. Geosciences 8:275

49. Saha A, Patil M, Goyal VC, Rathore DS (2018) Assessment and Impact of soil moisture index in Agricultural drought estimation using remote sensing and GIS techniques. Proc 7:2

50. Samanta S, Pal DK, Palsamanta B (2018) Flood susceptibility analysis through remote sensing, GIS and frequency ratio model. Appl Water Sci 8:66

51. Saaty TL (1990) How to make a decision: The analytic hierarchy process. Eur J Oper Res 48:9–26

52. Shiru MS, Johnson LM, Ujih OU, AbdulAzeez OT (2015) Managing flood in Ilorin, Nigeria: Structural and non structural measures. Asian J Appl Sci 3(5):507–513

53. Shuaibu A, Hounkpè J, Bossa YA, Kalin RM (2022) Flood risk assessment and mapping in the Hadejia River Basin, Nigeria, using Hydro-Geomorphic approach and multi-criterion decision-making method. Water 14:3709

54. Tella A, Balogun AL (2020) Ensemble fuzzy MCDM for spatial assessment of flood susceptibility in Ibadan, Nigeria. Nat Hazards 104:2277–2306

55. Tiepolo M, Rosso M, Massazza G, Belcore E, Issa S, Braccio S (2019) Flood assessment for risk-informed planning along the Sirba River, Niger. Sustainability 11:4003

56. Tokunbo A, Ezigbo B (2012) Floods claims 363 lives, displaced 2.1 million people says NEMA THISDAY. Available at http//Allafrican.com. Accessed 17 May 2014

57. UN-Water (2011) Cities coping with water uncertainties. Media Brief. UN-Water Decade Programme on Advocacy and Communication. Available at https://www.un.org/waterforlifedecade/pdf/unwdpac_biennial_report_2010_2011.pdf Accessed 12 Feb 2021

58. Usman M, Liedl R, Shahid MA, Abbas A (2015) Land use/land cover classification and its change detection using multi-temporal MODIS NDVI data. J Geogr Sci 25(12):1479–1506

59. Wang L, Qu J (2009) Satellite remote sensing applications for surface soil moisture monitoring: A review. Front Earth Sci China 3:237–247

60. Wang Y, Hong H, Chen W, Li S, Pamučar D, Gigovic L, Drobnjak S, Bui DT, Duan H (2019) A hybrid GIS multi-criteria decision-making method for flood susceptibility mapping at Shangyou, China. Remote Sens 11:62